Intramolecular C–H oxidative addition to iridium(I) in complexes containing a *N,N′*–diphosphanosilanediamine ligand.

Vincenzo Passarelli,[a] Jesús J. Pérez–Torrente,[b] Luis A. Oro.[b]*

[a] Centro Universitario de la Defensa, Ctra. Huesca s/n, ES–50090 Zaragoza, Spain;

[b] ISQCH–Universidad de Zaragoza, C/ Pedro Cerbuna s/n, ES–50009 Zaragoza, Spain.

Abstract[‡]

The iridium(I) complexes of formula Ir(cod)(SiNP)$^+$ (**1**$^+$) and IrCl(cod)(SiNP) (**2**) are easily obtained from the reaction of $SiMe_2\{N(4\text{–}C_6H_4CH_3)PPh_2\}_2$ (SiNP) with $[Ir(cod)(CH_3CN)_2]^+$ or $[IrCl(cod)]_2$, respectively. The carbonylation of [**1**][PF_6] affords the cationic pentacoordinated complexes [Ir(CO)(cod)(SiNP)]$^+$ (**3**$^+$) while the treatment **2** with CO gives the cation **3**$^+$ as an intermediate finally affording an equilibrium mixture of IrCl(CO)(SiNP) (**4**) and the hydride derivative of formula IrHCl(CO)(SiNP-H) (**5**) resulting from the intramolecular oxidative addition of the C–H bond of the $SiCH_3$ moiety to the iridium(I) center. Furthermore, the prolonged exposure of [**3**]Cl or **2** to CO resulted in the formation of the iridium(I) pentacoordinated complex Ir(SiNP–H)$(CO)_2$ (**6**). The unprecedented κ^3*C,P,P'* coordination

‡ The following abbreviations are used: cod, 1,5–cyclooctadiene; SiNP, $SiMe_2\{N(4\text{–}C_6H_4CH_3)PPh_2\}_2$; [SiNP–H], $Si(CH_2)(CH_3)\{N(4\text{–}C_6H_4CH_3)PPh_2\}_2$.

mode of the [SiNP–H] ligand observed in **5** and **6** has been fully characterized in solution by NMR spectroscopy. In addition, the single crystal X–ray structure of **6** is reported.

Introduction

The design of novel ligands and/or the modification of known ones is a well established strategy generally adopted in order to tune the electronic and steric properties at the coordinated metal center. In this relationship, the design of phosphano ligands containing P–N bonds has attracted a lot of interest, due to the easy functionalization and/or modification of the ligand backbone and to the consequent great versatility of these ligands both in coordination chemistry and in the study of stoichiometric and catalytic reactions.[1] Relevant to this paper, Scheme 1 shows selected diphosphano ligands containing the P–N functionality and different backbones and/or linkers. Interestingly, recently the coordination ability of $SiMe_2[(C_5H_4N–2)NPPh_2]_2$ ($SiN^{py}P$)[2] towards several transition metals has been described, and we have reported the synthesis of $SiMe_2\{N(4–C_6H_4CH_3)NPPh_2\}_2$ (SiNP)[3] and its reactivity towards rhodium. In spite of the differences in the electronic and steric features of both $SiN^{py}P$ and SiNP with respect to aliphatic diphosphanes like 1,2–bis(diphenylphoshano)ethane and 1,3–bis(diphenylphoshano)propane, both ligands always exhibit the expected $\kappa^2 P,P'$ coordination to the metal centre (Scheme 1).

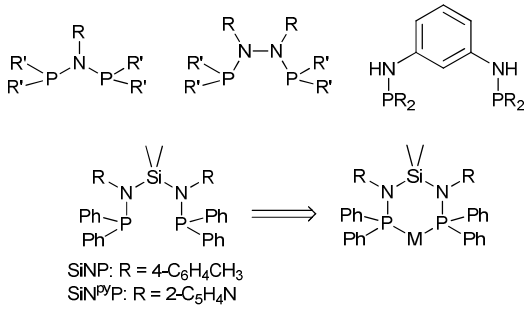

Scheme 1

As far as SiNP in combination with rhodium is concerned, Scheme 2 shows selected examples of complexes featuring the κ^2*P,P'* coordination mode of SiNP.[3]

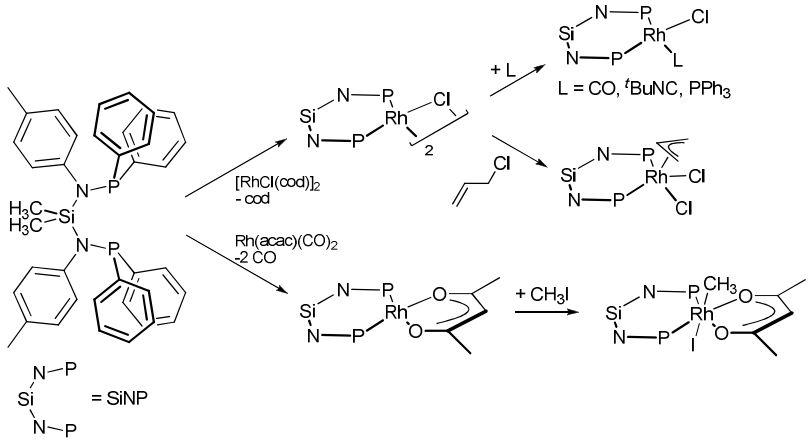

Scheme 2

On this background, we describe herein the preparation and characterization of novel iridium(I) complexes with SiNP along with the study of their reactivity. On one hand, it has been confirmed the predictable ability of SiNP to act as a bidentate κ^2*P,P'* ligand and, on the other, it has been observed the unprecedented easy intramolecular oxidative addition of the $SiCH_2$–H bond to the iridium(I) center with the consequent formation of the [SiNP–H] ligand featuring a κ^3*C,P,P'* coordination mode.

Results and discussion

Synthesis of iridium(I) complexes

The iridium(I) complexes $[Ir(cod)(SiNP)]^+$ (**1**$^+$) and IrCl(cod)(SiNP) (**2**) (Scheme 3) have been obtained by reaction of SiNP with $[Ir(cod)(CH_3CN)_2][PF_6]$ or $[IrCl(cod)]_2$, respectively (Scheme 3).

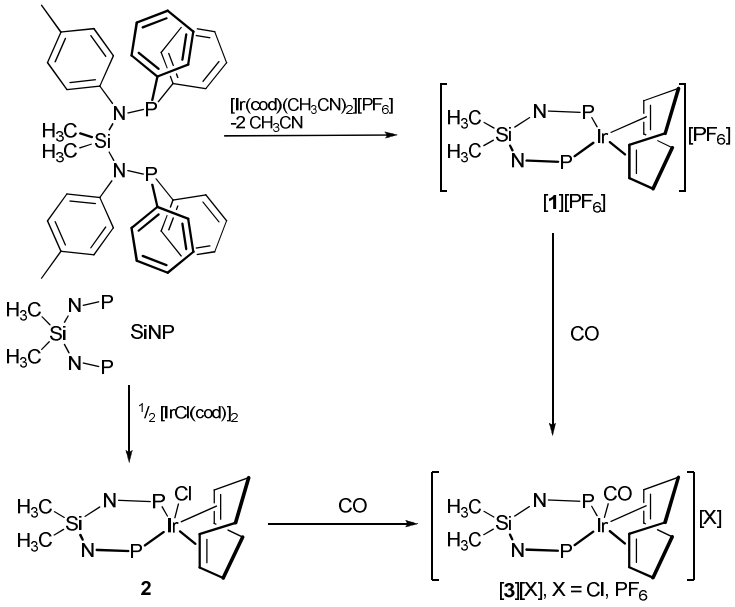

Scheme 3

In agreement with a square planar geometry at the metal center of $[Ir(cod)(SiNP)]^+$ ($\mathbf{1}^+$), the $^{31}P\{^1H\}$ NMR spectrum of $\mathbf{1}^+$ shows one singlet at 53.5 ppm for the SiNP ligand, and both equivalent tolyl groups and equivalent olefinic protons are observed (^1H, ^{13}C). Additionally the ^1H and $^{13}C\{^1H\}$ NMR spectra shows equivalent $SiCH_3$ moieties both at room temperature and at 183 K. On these bases both the *left* and *right* and the *up* and *down* semispaces at the cod and the SiNP ligands (Fig. 1) should be equivalent or eventually averaged by a fluxional process.

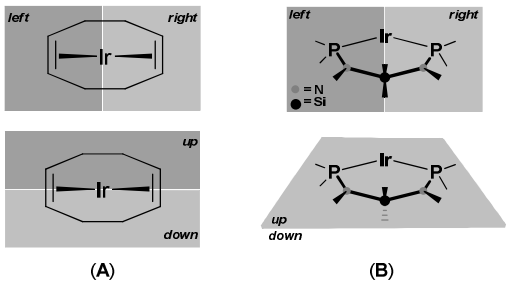

Fig. 1. Definition of the *left* and *right* and the *up* and *down* semispaces at the coordinated cod (A) and the coordinated SiNP (B) ligands.

In agreement with the above mentioned proposal, the optimized structures **1a**$^+$ and **1b**$^+$ of the cation [Ir(cod)(SiNP)]$^+$ (**1**$^+$) shows a slightly distorted square planar arrangement at the metal center with either a boat or a chair conformation of the SiN_2P_2Ir ring, respectively (Fig. 2). The free energy difference between the two structures is 9.4 kJ·mol^{-1}, the boat conformation being more stable than the chair one. Thus, the equivalence of the $SiCH_3$ methyls in **1**$^+$ should be reasonably the consequence of the fast reversible interconversion **1a**$^+$⇆**1b**$^+$.

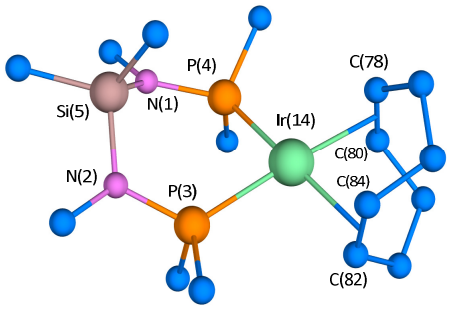

1a$^+$

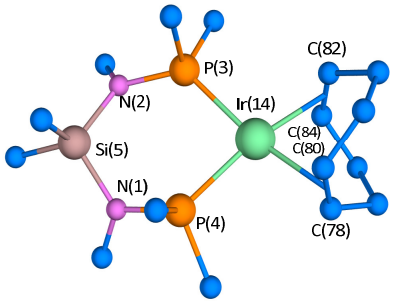

1b$^+$

Fig. 2. Optimized structures of [Ir(cod)(SiNP)]$^+$ (**1**$^+$) featuring a boat (**1a**$^+$) and a chair (**1b**$^+$) conformation at the SiN_2P_2Ir six-membered ring. Hydrogen atoms are omitted and only *ipso* carbon atoms of the aromatic rings are shown for clarity (see ESI for atomic coordinates). Selected bond distances of the boat (normal type) and the chair (italics type) conformers (Å) are in order: Ir(14)–C(78), 2.248, *2.343*; Ir(14)–C(80) 2.236, *2.226*; Ir(14)–C(82) 2.235, *2.285*; Ir(14)–C(84) 2.279, *2.225*; Ir(14)–P(3) 2.413, *2.379*; Ir(14)–P(4), 2.380, *2.356*; C(78)–C(80) 1.405, *1.394*; C(82)–C(84) 1.398, *1.403*.

For the pentacoordinated iridium compound IrCl(cod)(SiNP) (**2**) an apparent symmetric environment at the metal centre has been observed at room temperature. Indeed, similar to $\mathbf{1}^{+}$, one singlet at 49.4 ppm is observed in its $^{31}P\{^{1}H\}$ NMR spectrum and the ^{1}H NMR spectrum indicates equivalent olefinic protons of the cod ligand and equivalent tolyl groups (*cf.* Experimental). Further, at room temperature **2** shows a sharp ^{1}H singlet at 0.39 ppm for the $SiCH_3$ protons and, even at 183 K, the ^{1}H and $^{31}P\{^{1}H\}$ NMR spectra are similar to those at room temperature, the only difference being slightly broader signals. Thus, the *up* and *down* and the *left* and *right* semispaces (Fig. 1) both at the SiNP and at the cod ligands should be equivalent or averaged by a fluxional process. Starting from the ideal pentacoordinated configurations for IrCl(cod)(SiNP) shown in Fig. 3, optimized structures of **2** were calculated by means of standard computational methods and the minimum free energy structure was found to be that derived from the SPY–5–13 configuration, *i.e.* a square pyramid containing the chlorido ligand at the apical position (Fig. 4). Interestingly this arrangement was previously observed in the solid state structure of IrCl(cod)(dppb)[4] and IrCl(cod)(dppp)[5].

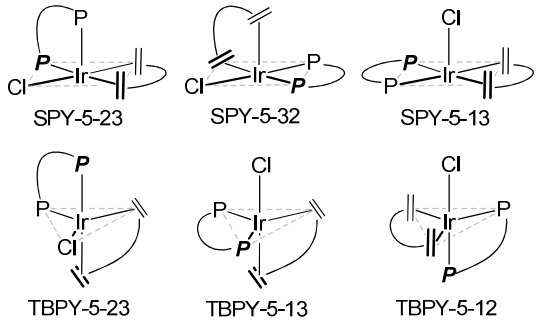

Fig. 3. Pentacoordinated ideal configurations for IrCl(cod)(SiNP) (**2**).

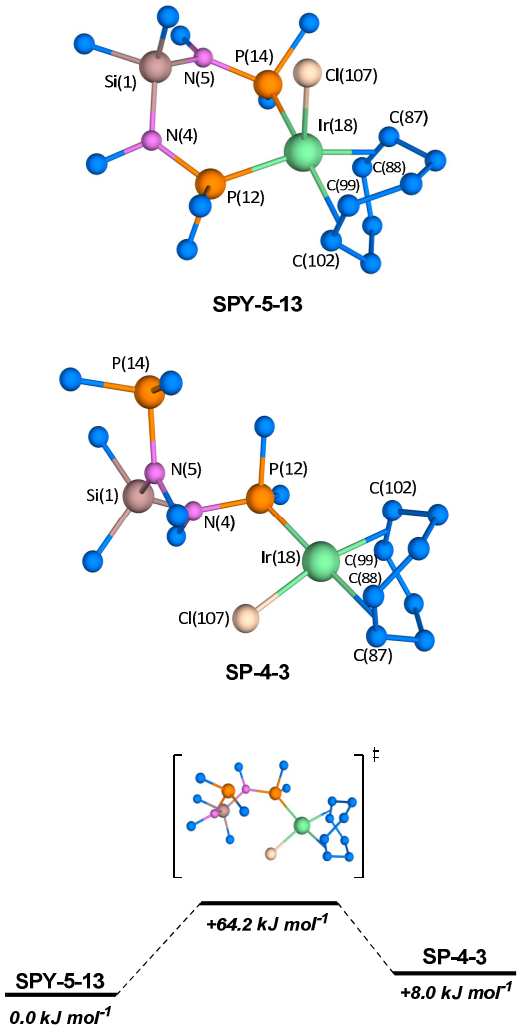

Fig. 4. Optimized SPY–5–13 and SP–4–3 structures of **2** and the reaction profile for the equilibrium SP–5–13⇆SP–4–3. Hydrogen atoms are omitted and only *ipso* carbon atoms of the aromatic rings are shown for clarity (see ESI for atomic coordinates). Selected bond distances of **2** with the SPY–5–13 (normal type) and SP–4–3 (italics type) configurations (Å) are in order: Ir(18)–P(12), 2.393, *2.371*; Ir(18)–P(14), 2.407, *n.d.*; Ir(18)–C(87), 2.164, *2.234*; Ir(18)–C(88), 2.185, *2.188*; Ir(18)–C(99), 2.181, *2.166*; Ir(18)–C(102). 2.225, *2.132*; Ir(18)–Cl(107), 2.567, *2.382*; C(87)–C(88), 1.435, *1.402*; C(99)–C(102), 1.420, *1.428*.

The optimized SPY–5–13–structure of **2** features *nonequivalent up* and *down* semispaces both at the SiNP and the cod ligands but, as mentioned before, *equivalent up* and *down* semispaces

(both at cod and SiNP) were observed for **2** even at 183 K, thus a fluxional process exchanging the above mentioned semispaces should be operative. In this relationship, it is noteworthy that the other optimized structures of **2**, *i.e*. those derived from the SPY–5–32, SPY–5–23, TBPY–5–23, TBPY–5–12 and TBPY–5–13 configurations, Fig. 3, were found to be significantly less stable than the SPY–5–13 one with relative free energies higher than 65 $kJ \cdot mol^{-1}$. Thus the *up-down* exchange *via* the reversible interconversion between different pentacoordinated structures can be ruled out. Furthermore the gas phase ΔG^0 values for the formation of a square planar complex *via* the dissociation from the metal either of the chlorido ligand (ΔG^0 = 459 $kJ \cdot mol^{-1}$) or of one doble bond of the cod ligand (ΔG^0 = 122 $kJ \cdot mol^{-1}$) clearly indicate that none of the above mentioned dissociation equilibria can be proposed in order to justify the observed exchange. On the other hand, the small free energy difference (+8.0 $kJ \cdot mol^{-1}$) between the optimized tetracoordinate square complex (SP–4–3) shown in Fig. 4 and the SPY–5–13 structure and the affordable activation barrier calculated for the equilibrium SPY–5–13⇆SP–4–3 ($\Delta H^{\ddagger}$ = 68.8 $kJ \cdot mol^{-1}$; $\Delta S^{\ddagger}$ = 15.4 $J \cdot mol^{-1} \cdot K^{-1}$) suggest that the reversible dissociation of one phosphorus atom from the metal center should be the process averaging the semispaces both at the cod and at the SiNP ligands.

CO–promoted C–H activation

The irreversible carbonylation of $[Ir(cod)(SiNP)]^+$ ($\mathbf{1}^+$) and IrCl(cod)(SiNP) (**2**) is fast and complete under mild conditions (1 atm of CO, room temperature, aprox. 10 min) resulting in the formation of the pentacoordinated cation of formula $Ir(CO)(cod)(SiNP)^+$ ($\mathbf{3}^+$) isolated as both [**3**]Cl and [**3**][PF_6], depending on the starting complex used in the synthesis (Scheme 3).

The IR spectrum of $\mathbf{3}^+$ (CH_2Cl_2 solutions) shows a strong ν_{CO} absorption at 1994 cm^{-1} in agreement with the presence of the coordinated CO ligand. At room temperature the ^1H NMR

spectrum of $\mathbf{3}^+$ shows nonequivalent $SiCH_3$ groups thus indicating that there exist nonequivalent *up* and *down* semispaces at SiNP (Fig. 1). Further, equivalent phosphorus nuclei (^{31}P) and tolyl groups (^1H and ^{13}C) are observed at room temperature while at 183 K the $^{31}P\{^1H\}$ NMR spectrum of $\mathbf{3}^+$ shows two signals (δ_P = 41.2, 37.3 ppm, *cf.* ESI) and accordingly two methyl ^1H resonances at 2.20 and 2.04 ppm for the tolyl moieties, as well. Thus besides the *up* and *down* nonequivalence at the SiNP ligand observed at room temperature, also nonequivalent *left* and *right* semispace should exist, and therefore a fluxional process should exchange them at room temperature (*vide infra*).

As far as the cod ligand is concerned, its olefinic protons are totally equivalent at room temperature, that is only one ^1H resonance is observed at 3.86 ppm, but at 183 K the ^1H NMR spectrum of $\mathbf{3}^+$ shows four olefinic resonances (δ_H = 4.25, 3.20, 1.80 and 1.30 ppm, *cf.* ESI for the assignment) indicating that both the *up* and *down* and the *left* and *right* semispaces at the cod ligand of $\mathbf{3}^+$ are nonequivalent at that temperature, and that the observed equivalence at room temperature results from a fluxional process averaging the above mentioned semispaces. The possible ideal configurations which match the NMR spectroscopic data are shown in Fig. 5 (SPY–5–12, SPY–5–23, TBPY–5–12) along with the optimized TBPY–5–12 structure which was found to be the minimum free energy one.[6] Noteworthy, similar to $\mathbf{1}^+$ and **2**, in the minimum free energy structure the boat conformation of the SiN_2P_2Ir ring was found to be more stable than the chair one (+16.6 $kJ \cdot mol^{-1}$).

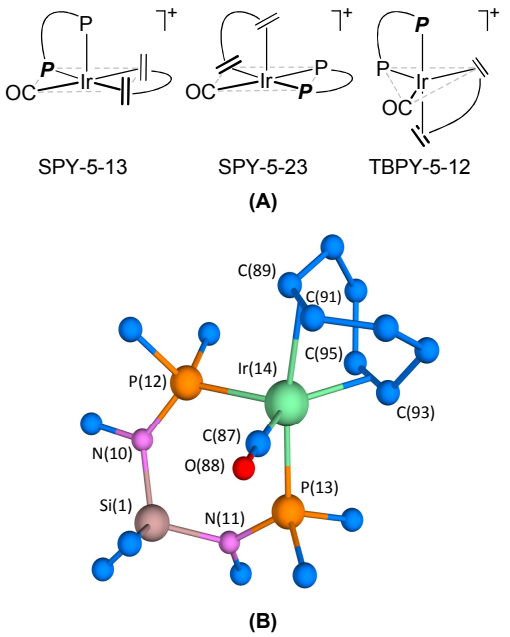

Fig. 5. (A) Selected ideal configurations for $[Ir(CO)(cod)(SiNP)]^+$ ($\mathbf{3}^+$). (B) Optimized TBPY–5–12 structure of $\mathbf{3}^+$. Hydrogen atoms are omitted and only *ipso* carbon atoms of the aromatic rings are shown for clarity (for atomic coordinates see ESI). Selected bond distances (Å) are in order: Ir(14)–C(87), 1.922; Ir(14)–C(89), 2.361; Ir(14)–C(91), 2.345; Ir(14)–C(93), 2.177; Ir(14)–C(95), 2.196; Ir(14)–P(12), 2.518; Ir(14)–P(13), 2.428; C(87)–C(88), 1.155.

As far as the possible fluxional processes affecting both the cod and the SiNP ligands are concerned, the nature of the ^{1}H NMR spectra (*cf.* ESI) prevented both the ^{1}H line shape analysis and the quantitative analysis of ^{1}H–^{1}H EXSY spectra at different temperatures. Nevertheless the line shape analysis of the ^{31}P{^{1}H} resonances was easily carried out in the range 183–223 K affording the kinetic constants for the exchange of the *left* and *right* semispaces at the SiNP ligand. The activation parameters obtained from the Eyring plot ($\Delta H^{\ddagger}$ = 50.1±0.5 kJ·mol^{-1}; $\Delta S^{\ddagger}$ = 44.3±2.6 J·mol^{-1}·K^{-1}, *cf.* ESI) and the fact that the exchange of the methyls of the $Si(CH_3)_2$ moiety is not observed reasonably indicate that the mechanism for the *left–right* exchange at the SiNP ligand is nondissociative. In this respect, it is worth mentioning that

besides the TBPY–5–12 configuration, the TBPY–5–23 and the SPY–5–32 structures shown in Fig. 6A were found to be local minima in the potential free energy surface, being located at +25.7 and +27.5 kJ·mol^{-1}, respectively, with respect to the TBPY–5–12 structure. Thus the equilibria TBPY–5–12⇆SPY–5–32 and/or TBPY–5–12⇆TBPY–5–23 (Fig. 6B) should be operative in solution and could be responsible for the *left–right* exchange at the SiNP ligand.

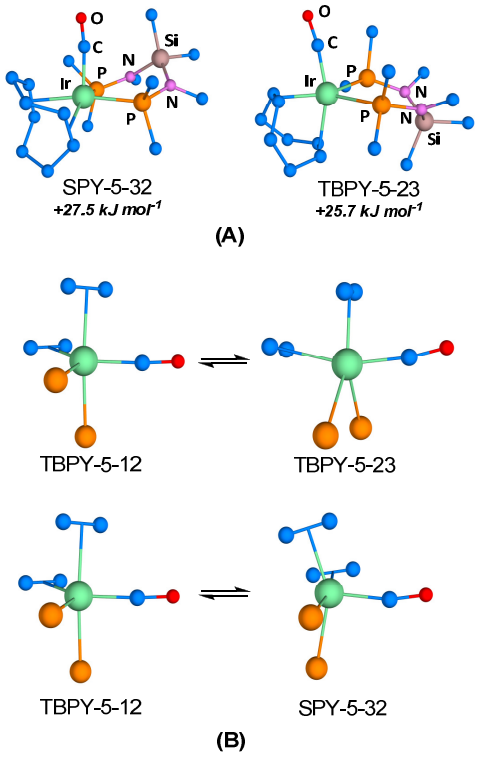

Fig. 6. (A) Optimized SPY–5–32 and TBPY–5–23 structures of [Ir(CO)(cod)(SiNP)]$^+$ (**3**$^+$) with the relative free energies given with respect to TBPY–5–12. (B) Representation of the TBPY–5–12⇆SPY–5–32 and TBPY–5–12⇆TBPY–5–23 equilibria emphasizing the changes in the coordination sphere of the metal center.

Additionally, it is worth mentioning that these equilibria exchange the *up* and *down* (TBPY–5–12⇆TBPY–5–23) and the *left* and *right* (TBPY–5–12⇆SPY–5–32) semispaces at the cod ligand as well, thus reasonably they account also for the dependence on the temperature of the ^{1}H pattern of the cod ligand.

Solutions of [**3**]Cl are thermally unstable and the complete conversion of [**3**]Cl is observed in approximately 6 hours affording a mixture of IrCl(CO)(SiNP) (**4**) and IrHCl(CO)(SiNP–H) (**5**) with a molar ratio of 4:1, regardless of the concentration of [**3**]Cl. The ^{1}H and $^{31}P\{^{1}H\}$ NMR measurements indicate that at the beginning of the transformation of [**3**]Cl, the cod ligand is released and **4** is cleanly formed, no intermediate being detected even at 253 K. In addition, after approximately 15 min from the formation of **4**, measurable quantities of **5** are observed in the ^{1}H and $^{31}P\{^{1}H\}$ NMR spectra as the consequence of the activation of one C–H bond of the $SiCH_3$ group (Scheme 4).

Interestingly the CH_2Cl_2 solutions of [**3**][PF_6] are thermally stable and the addition of equimolar amounts of [PPN]Cl resulted in the formation of the mixture **4**+**5** (4:1 molar ratio), as well. When the reaction was carried out changing the molar ratio $Cl^-/\mathbf{3}^+$ (from 0.5 to 2) the same products, *i.e.* **4** and **5**, and the same molar ratio between them, *i.e.* 4:1, were observed.

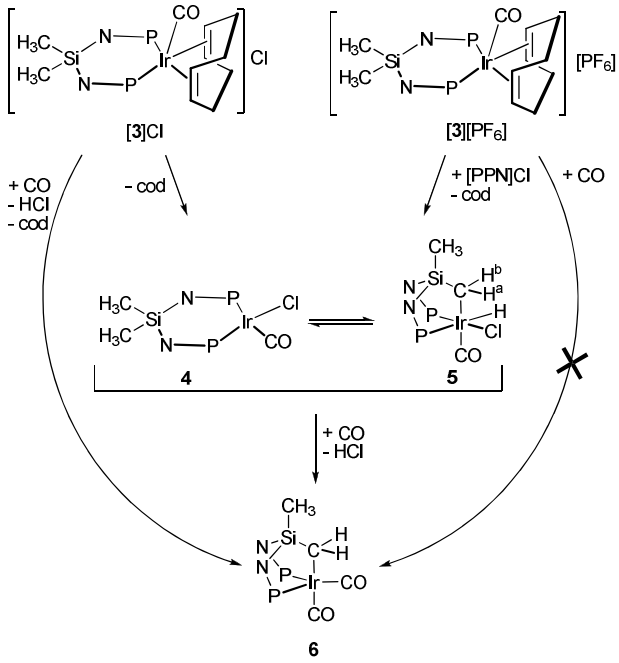

Scheme 4

The IR spectrum of a CH_2Cl_2 solution of the mixture **4**+**5** shows absorptions at 2007 (**4**) and 2026 cm^{-1} (**5**) indicating the presence of two species each containing coordinated carbon monoxide. The NMR spectra of **4** suggests a square planar coordination of the metal center. Indeed two nonequivalent phosphorus atoms are observed with the expected coupling constants for a *cis* arrangement ($^2J_{PP}$ = 30.5 Hz), and a $^{13}C\{^1H\}$ doublet–of–doublets is observed at 181.3 ppm ($^2J_{PC}$ = 124.3, 11.1 Hz) confirming that the CO ligand occupies the *trans* position with respect to one phosphorus and a *cis* one with respect to the other one. In agreement with the proposed arrangement of the donor atoms at the metal center of **4**, the tolyl groups are not equivalent (*cf*. Experimental). As a confirmation the optimized structure of **4** features a square planar arrangement of the donor atoms at the metal center and, similar to $\mathbf{1}^+$, **2** and $\mathbf{3}^+$, the boat conformation of the SiN_2P_2Ir ring is calculated to be slightly more stable (6.4 $kJ \cdot mol^{-1}$) than the chair one (Fig. 7). In this connection the interconversion between the two conformers should be responsible for the observed equivalence between the $SiCH_3$ methyls.

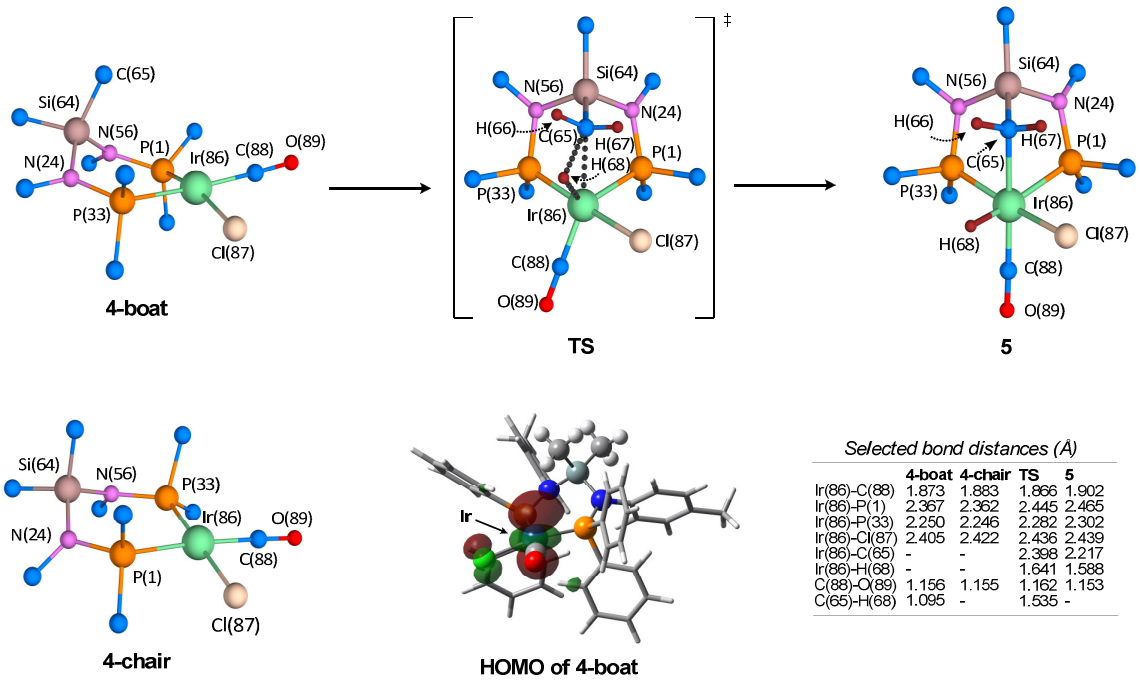

Selected bond distances (Å)

	4-boat	4-chair	TS	5
Ir(86)-C(88)	1.873	1.883	1.866	1.902
Ir(86)-P(1)	2.367	2.362	2.445	2.465
Ir(86)-P(33)	2.250	2.246	2.282	2.302
Ir(86)-Cl(87)	2.405	2.422	2.436	2.439
Ir(86)-C(65)	-	-	2.398	2.217
Ir(86)-H(68)	-	-	1.641	1.588
C(88)-O(89)	1.156	1.155	1.162	1.153
C(65)-H(68)	1.095	-	1.535	-

Fig. 7. Optimized structures of IrCl(CO)(SiNP) (**4**), IrHCl(CO)(SiNP–H) (**5**) and the transition state for the transformation **4**⇆**5** along with the calculated HOMO of the boat conformer of **4**. Selected bond distances (Å) are given in the table and selected angles (°) are in order: C(65)–Ir(86)–C(88), 175.1 (**5**), 152.0 (**TS**); C(65)–Ir(86)–Cl(87), 89.5 (**5**), 92.2 (**TS**). Hydrogen atoms are omitted and only *ipso* carbon atoms of the aromatic rings are shown for clarity (for atomic coordinates see ESI).

When dealing with **5**, the spectroscopic data clearly indicates the presence of a hydride moiety and of the [SiNP–H] ligand featuring a κ^3*C,P,P'* coordination mode, both resulting from the intramolecular $SiCH_2$–H oxidative addition to the iridium(I) center of **4**. The $^{31}P\{^1H\}$ and $^{13}C\{^1H\}$ NMR spectra (*cf.* ESI) point unambiguously at the presence of two mutually *cis* phosphorus nuclei (δ_P = 48.1, 43.0 ppm, $^2J_{PP}$ = 9.0 Hz) with the carbon of the CO ligand *cis* to both of them ($^{13}C\{^1H\}$ triplet at 172.48 ppm, $^2J_{PC}$ = 4.5 Hz). On the other hand, the coupling constants $^2J_{HP}$ of the hydride ligand (δ_H = –9.11 ppm) indicate that it occupies a *cis* position to one phosphorus ($^2J_{HP}$ = 18.0 Hz) and the *trans* one to the other ($^2J_{HP}$ = 177.9 Hz) (*cf.* ESI). Finally, the methylene carbon atom of the activated $SiCH_3$ group occupies a *cis* position with respect to both phosphorus atoms and the coordination sphere of iridium should be completed by one chlorido ligand. In agreement with the proposed structure, nonequivalent

tolyl groups (*cf*. Experimental) and nonequivalent methylenic hydrogen atoms are observed (δ_H = 0.79, H^a, 1.40 ppm, H^b). Further, the ^1H resonances for H^a and H^b show a pattern clearly indicating that H^b should feature a smaller dihedral angle with respect to the hydride moiety than H^a (Scheme 4, *cf*. ESI). Indeed the scalar coupling constant of H^b with the hydride is 3.0 Hz, while no scalar coupling was observed between H^a and the hydrogen of the Ir–H moiety (*cf*. ESI). Since the Karplus curve for a H–X–Y–H system generally features a local maximum at the dihedral angle H–X–Y–H of 0º and a local minimum at near 90º, the dihedral angle H^a–C–Ir–H should be close to 90º.[7]

As a confirmation, the proposed structure of **5** was optimized by standard computational methods (Fig. 7) and was found to feature a distorted octahedral arrangement of the donor atoms at the metal center with H^x–C–Ir–H dihedral angles of 100º (x = a) and 16º (x = b) in agreement with the above mentioned $^3J_{HH}$ coupling constants. Additionally, it is worth mentioning that the calculated ν_{CO} wave numbers (**4**, 2017; **5**, 2029 cm^{-1}) are found close to the experimental ones (**4**, 2007; **5**, 2026 cm^{-1}).

Finally the transition state structure for the transformation **4⇆5** was calculated showing that the boat conformer of **4** allows the C–H bond to approach the metal–centered HOMO shown in Fig. 7. Consequently the synchronous cleavage of the $SiCH_2$–H bond (1.535 Å) and formation of the Ir–CH_2Si (2.398 Å) and Ir–H (1.641 Å) bonds takes place along with shift of the CO ligand from the equatorial plane to the axial position.

The treatment of a solution of **4**+**5** with CO (1 atm, 12 h) yields the formal elimination of HCl and the quantitative formation of the pentacoordinated iridium(I) dicarbonyl complex **6** still featuring the metallated [SiNP–H] ligand (Scheme 4).[8] The solid state structure of **6** has been

determined by single crystal X–ray diffraction and its molecular structure is shown in Fig. 8. Tab. 1 contains selected bond distances and angles.

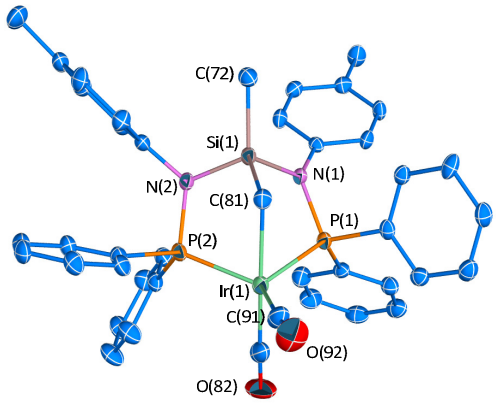

Fig. 8. ORTEP views of Ir(SiNP–H)$(CO)_2$ (**6**) with the numbering scheme adopted and the thermal ellipsoids at 50% probability.

Tab. 1. Selected bond angles (º) and distances (Å) of Ir(SiNP–H)$(CO)_2$ (**6**).

Ir(1)–C(81) 1.885(5)	N(1)–C(51) 1.418(4)
Ir(1)–C(91) 1.885(5)	N(2)–C(61) 1.441(4)
Ir(1)–C(71) 2.185(4)	C(81)–O(82) 1.135(5)
Ir(1)–P(1) 2.290(2)	C(91)–O(92) 1.145(5)
Ir(1)–P(2) 2.3100(19)	C(71)–Si(1)–C(72) 120.59(17)
P(1)–N(1) 1.691(3)	C(81)–Ir(1)–C(91) 100.09(19)
P(1)–C(11) 1.811(4)	C(81)–Ir(1)–C(71) 173.53(16)
P(1)–C(21) 1.815(4)	C(91)–Ir(1)–C(71) 85.91(16)
P(2)–N(2) 1.701(3)	C(81)–Ir(1)–P(1) 95.34(13)
P(2)–C(41) 1.809(4)	C(91)–Ir(1)–P(1) 120.10(13)
P(2)–C(31) 1.823(4)	C(71)–Ir(1)–P(1) 79.45(11)
Si(1)–N(2) 1.756(3)	C(81)–Ir(1)–P(2) 95.29(13)
Si(1)–N(1) 1.766(3)	C(91)–Ir(1)–P(2) 128.67(14)
Si(1)–C(71) 1.830(4)	C(71)–Ir(1)–P(2) 82.65(10)
Si(1)–C(72) 1.842(4)	P(1)–Ir(1)–P(2) 106.61(7)

The [SiNP–H] ligand features a tridentate κ^3*C,P,P'* coordination mode involving both the two phosphorus atoms and the carbon atom of the $SiCH_2$ moiety. Interestingly reasonably due to the presence of two fused five–membered rings, namely Ir(1)–P(1)–N(1)–Si(1)–C(71) and Ir(1)–P(2)–N(2)–Si(1)–C(71), the P(1), P(2) and C(71) atoms show a distorted *fac* arrangement at the metal centre with an expanded P(1)–Ir(1)–P(2) angle (106.61º) and compressed P(1)–Ir(1)–C(71) and P(2)–Ir(1)–C(71) angles (79.45º, 82.65º) with respect to the

ideal 90º value. The coordination sphere at the metal centre is completed by two CO ligands, one occupying the position *trans* to C(71) and the other in the equatorial plane of the molecule, the overall coordination polyhedron being a distorted trigonal bypiramid (TBPY–5–23). With this respect it is worth mentioning that Ir(1) lays approximately 0.3 Å out of the equatorial plane, slightly shifted towards the C(81) atom. As far as bond distances are concerned, related structurally characterized iridium(I) complexes, such as $Ir\{C_6H_3(CH_2P(CF_3)_2)_2\}(CO)_2$[9] and $Ir(CF_2CF_2H)(CO)_2(PPh_3)_2$[10] feature similar Ir–C–O, Ir–P and Ir–C bond distances, although with different coordination polyhedra or ligands' distribution around the metal center. On the other hand, the Si(1)–C(71) and Si(1)–C(72) are very similar to the silicon–carbon bond distances observed in $RhCl_2(\eta^3\text{–}C_3H_5)$(SiNP) (1.854; 1.839 Å).[3] Nevertheless a severe distortion of the C–Si–C angle is observed. Indeed the C–Si–C angle in $RhCl_2(\eta^3\text{–}C_3H_5)$(SiNP) is 108.02º whereas the C(71)–Si(1)–C(72) angle in Ir(SiNP–H)$(CO)_2$ is 120.59º thus suggesting that the coordination of the methylene moiety to iridium entails a significant expansion of the C–Si–C angle. For the sake of comparison, it should be mentioned that when comparing angles and bond distances of the $[IrP_2(CH_2)(CO^{ax})]$ moiety in the calculated structure of **5** with that in the solid state structure of **6**, very small differences (≤3%) were observed, mayor deviations being observed only for one of the two Ir–P bond distances (namely that for the phosphorus *trans* to the hydride ligand in **5**) and the P–Ir–P angle (wider in **6** due to the less congested coordination sphere at the metal center).

Finally, the solid state structure of **6** is maintained in solution. Indeed two IR absorptions (CH_2Cl_2) were observed at 1927 and 2001 cm^{-1} (ν_{CO}) in agreement with the presence of a Ir$(CO)_2$ moiety in an environment of C_s symmetry. Further, the ^1H, $^{13}C\{^1H\}$ and $^{31}P\{^1H\}$ NMR

spectra indicate a *fac* symmetrically coordinated [SiNP–H] ligand, *i.e.* both the two N–P arms of the ligand and the protons of the $IrCH_2$ moiety are equivalent (*cf.* Experimental).

In relation to the C–H activation in the coordinated SiNP ligand, it is worth mentioning that, to the best of our knowledge, the intramolecular C–H addition of a methyl moiety from a coordinated diphosphane ligand to a Group 10 metal has previously been reported only in rhodium complexes containing the ligands $1,3–(CH_2P^tBu_2)_2(C_6H_4)$ or $1,3–(CH_2P^tBu_2)–4,6–(CH_3)_2(C_6H_2)$.[11] The ability of both diphosphano ligands to adopt a *trans*–spanning coordination mode and their rigidity were found to be decisive in getting the CH_3 moiety close to the metal centre, and finally in promoting the addition of the C–H bond to the metal center (Chart 1).[11] On the contrary, SiNP tends to coordinate the metal center occupying two *cis* sites and the boat conformation of the SiN_2P_2Ir is the necessary requisite to allow the $SiCH_2$–H group to approach the metal center and finally add to the metal center.

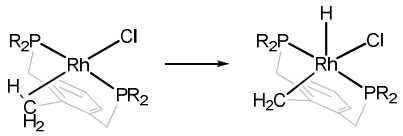

Chart 1

Conclusions

The *N,N'*–diphosphanosilanediamine ligand $SiMe_2\{N(4–C_6H_4CH_3)PPh_2\}_2$ (SiNP) is able to coordinate iridium(I) affording tetra– or pentacoordinated complexes (**1**$^+$, **2** and **3**$^+$). The solution structure of the pentacoordinated complexes of formula $[IrX(SiNP)(cod)]^{n+}$ (**2**, X = Cl, n = 0; **3**$^+$, X = CO, n = 1) depends on the nature of the ancillary ligand X. Indeed, the most sterically demanding chlorido ligand best fits the apical position of a square planar pyramid, while the trigonal bypiramydal structure is the most favored with the less hindered CO ligand, in both cases a boat conformation being adopted by the SiN_2P_2Ir ring. Different fluxional processes for **2**

and $\mathbf{3}^+$ are observed in solution as a consequence of the different geometries at the metal center: indeed the reversible dissociation of one phosphorus atom of the SiNP ligand in IrCl(cod)(SiNP) (**2**) was calculated to be the process averaging the *up* and *down* semispaces both at the cod and the SiNP ligands. On the other hand the interconversion(s) between pentacoordinated isomers should be responsible for the averaged ^{1}H and ^{31}P NMR spectra of $\mathbf{3}^+$ at room temperature.

Starting from the carbonyl species $[Ir(CO)(cod)(SiNP)]^+$ ($\mathbf{3}^+$) the C–H addition to the iridium(I) center easily takes place at room temperature when the chloride ion is present in solution, either as the counter–ion in [**3**]Cl or if added as [PPN]Cl to [**3**][PF_6]. Under these conditions the preliminary formation of the tetracoordinated carbonyl complex IrCl(CO)(SiNP) (**4**) has been observed along with the consequent formation of the hydride complex IrHCl(CO)(SiNP–H) (**5**) *via* the synchronous cleavage of the $SiCH_2$–H bond, the formation of the Ir–CH_2Si and Ir–H bonds, and the shift of the CO ligand from the equatorial plane in **4** to the axial coordination site in **5**.

Finally the κ^3*C,P,P'* coordination mode of the [SiNP–H] ligand has been fully characterized in the solid state in the pentacoordinated dicarbonyl iridium(I) complex Ir(SiNP–H)$(CO)_2$ (**6**) showing that it easily fits three mutually *cis* coordination sites and that a severe distortion of the C–Si–C angle is necessary in order to accommodate the methylene moiety in the coordination sphere of the metal center.

The influence of the ancillary ligands on the C–H bond activation and the application of the resulting Ir[κ^3*C,P,P'*–(SiNP–H)] platform to both stoichiometic and catalytic processes is being investigated and results will be published in due course.

Experimental section

All the operations were carried out using standard schlenk–tube techniques under an atmosphere of prepurified argon or in a Braun glove–box under dinitrogen or argon. The solvent were dried and purified according to standard procedures. [PPN]Cl (Aldrich) and CO (Praxair) were commercially available and were used as received. The compounds $[IrCl(cod)]_2$,[12] $[Ir(cod)(CH_3CN)_2][PF_6]$,[13] and SiNP[3] were prepared as previously described in the literature. NMR spectra were measured with Bruker spectrometers (AV300, AV400, AV500) and are referred to $SiMe_4$ (^1H, ^{13}C), H_3PO_4 (^{31}P) and $CFCl_3$ (^{19}F). The diffusion experiments were performed using the stimulated echo pulse sequence[14] without spinning and the collected data were treated as previously described.[3] The hydrodynamic radius (R_h) was calculated using the equation of Stokes–Einstein and the radius of gyration (R_g) was calculated according the literature, using optimized molecular structures.[15] Infrared spectra were recorded on a ThermoNicolet Avatar 360 FT–IR spectrometer. Elemental analyses were performed by using a Perkin–Elmer 2400 microanalyzer.

Synthesis of [Ir(cod)(SiNP)][PF$_6$] ([**1**][PF_6]). A solution of SiNP (150 mg, 0.235 mmol, 638.79 g/mol) in CH_2Cl_2 (10 mL) was added with $[Ir(cod)(CH_3CN)_2][PF_6]$ (124 mg, 0.235 mmol, 527.47 g/mol). After 30 min stirring, the resulting deep orange solution was evaporated and the resulting solid washed with hexane (3 x 5 mL). The deep orange solid was dried under vacuum and identified as $[Ir(cod)(SiNP)][PF_6]$ ([**1**][PF_6], 224 mg, 88% yield). Found: C, 53.02; H, 5.00; N, 2.52. Calcd for $C_{48}H_{52}F_6IrN_2P_3Si$ (1084.15): C, 53.18; H, 4.83; N, 2.58. ^1H NMR (CD_2Cl_2, 298 K): δ 7.30–7.51 (20H, PPh, δ_C = 128.2, *m*–PPh, 131.5, *p*–PPh, 133.7, *o*–PPh), 6.85 (d, 8.2 Hz, 4H, C^3H^{tol}, δ_C = 129.4), 6.68 (d, 8.2 Hz, 4H, C^2H^{tol}, δ_C = 129.6), 4.31 (br, 4H, $C^{sp2}H^{cod}$, δ_C = 88.6), 2.28–2.15 (10H, $C^{sp3}H^{cod}$ + CH_3^{tol}, δ_C = 20.4, CH_3^{tol}), 2.07 (m, 4H, $C^{sp3}H^{cod}$,

δ_C = 30.8), –0.67 (s, 6H, $SiCH_3$, δ_C = 3.7). ^{19}F NMR (CD_2Cl_2, 298 K): δ –73.5 (d, 710.5 Hz). $^{31}P\{^1H\}$ NMR (CD_2Cl_2, 298 K): δ 53.5 (s, SiNP), –144.4 (sp, 710.5 Hz, PF_6^-). *D* ($CDCl_3$, 298 K) = (5.94±0.03)·10^{-6} $cm^2 \cdot s^{-1}$, R_h = 6.45±0.03 Å (R_g = 6.33 Å)

*Synthesis of IrCl(cod)(SiNP)(**2**).* A suspension of SiNP (466 mg, 0.730 mmol, 638.79 g/mol) in CH_2Cl_2 (5 mL) was added with $[IrCl(cod)]_2$ (252 mg, 0.375 mmol, 671.70 g/mol). The mixture was stirred for 1 h and the resulting solid was filtered off, dried *in vacuo* and identified as IrCl(cod)(SiNP) (**2**, 498 mg, 70% yield). Found: C, 59.24; H, 5.33; N, 2.55. Calcd for $C_{48}H_{52}ClIrN_2P_2Si$ (974.64): C, 59.15; H, 5.38; N, 2.87. ^1H NMR ($CDCl_3$, 298 K): δ 7.62 (m, 4H, *o*–PPh, δ_C = 134.31), 7.31 (t, $^3J_{HH}$ = 7.1 Hz, 2H, *p*–PPh, δ_C = 129.84), 7.22 (t, $^3J_{HH}$ = 7.1 Hz, 4H, *m*–PPh, δ_C = 126.99), 6.69 (d, 7.4 Hz, 2H, C^3H^{tol}, δ_C = 128.69), 6.57 (d, 7.4 Hz, C^2H^{tol}, δ_C = 130.9), 3.42 (br, 2H, $C^{sp2}H^{cod}$, δ_C = 74.97), 2.25–2.06 (5H, CH_3^{tol} + $C^{sp3}H_2^{cod}$, δ_C = 20.74, CH_3^{tol}, 31.58, $C^{sp3}H_2^{cod}$), 1.74 (m, 2H, $C^{sp3}H_2^{cod}$), 0.39 (s, 3H, $SiCH_3$, δ_C = 4.21). ^{31}P NMR ($CDCl_3$, 298 K): δ 49.4 (s). *D* (CD_2Cl_2, 298 K) = (8.87±0.21)·10^{-6} $cm^2 \cdot s^{-1}$, R_h = 5.72±0.14 Å (R_g = 5.97 Å).

*Synthesis of [Ir(CO)(cod)(SiNP)][PF$_6$] ([**3**][PF$_6$]).* A solution of [Ir(cod)(SiNP)][PF_6] (156 mg, 0.144 mmol, 1084.15 g/mol) in CH_2Cl_2 (3 mL) was stirred under an atmosphere of CO (1 atm) for 20 min. A pale yellow solution was obtained which was partially evaporated and added with hexane (10 mL) affording a yellow solid identified as [Ir(CO)(cod)(SiNP)][PF_6] ([**3**][PF_6], 147 mg, 92% yield). Found: C, 53.01; H, 4.92; N, 2.48. Calcd for $C_{49}H_{52}F_6IrN_2OP_3Si$ (1112.16): C, 52.92; H, 4.71; N, 2.52. ν_{CO} (CH_2Cl_2), 1994 cm^{-1}. ^1H NMR (CD_2Cl_2, 298 K): δ 7.36–7.69 (PPh, 20H, δ_C = 134.98, *m*–PPh; 132.48, *m*–PPh; 128.31, *o*–PPh; 128.11, *o*–PPh; 132.12, *p*–PPh; 131.57 or 131.64, *p*–PPh), 6.97 (d, 8.2 Hz, 2H, C^3H^{tol}, δ_C = 129.54), 6.92 (d, 8.2 Hz, 2H, C^2H^{tol}, δ_C = 131.57 or 131.64), 6.77 (d, 8.2 Hz, 2H, C^3H^{tol}, δ_C = 129.34), 6.18 (d, 8.2 Hz, 2H, C^2H^{tol}, δ_C = 131.33), 3.86 (br, 4H, $C^{sp2}H^{cod}$, δ_C = 82.90), 2.22 (s, CH_3^{tol}, 3H, δ_C = 20.52),

2.05 (m, 4H, $C^{sp3}H^{cod}$, δ_C = 32.51), 1.93 (m, $C^{sp3}H^{cod}$, 4H, δ_C = 32.51), 0.56 (s, 3H, $SiCH_3$, δ_C = 1.24), –0.29 (s, 3H, $SiCH_3$, δ_C = 3.26). $^{13}C\{^1H\}$ NMR (CD_2Cl_2, 298 K): δ 179.4 (t, 4.6 Hz, CO). $^{31}P\{^1H\}$ NMR (CD_2Cl_2, 298 K): δ 39.4 (s, SiNP), –144.4 (sp, 710.5 Hz, PF_6^-). *D* (CD_2Cl_2, 298 K) = (7.89±0.06)·10^{-6} $cm^2 \cdot s^{-1}$, R_h = 6.43±0.04 Å (R_g = 6.31 Å).

Reaction of IrCl(cod)(SiNP) with CO. a) Synthesis of [Ir(CO)(cod)(SiNP)]Cl ([**3**]Cl). A suspension of IrCl(cod)(SiNP) (159 mg, 0.163 mmol, 974.64 g/mol) in CH_2Cl_2 (5 mL) was degassed and contacted with CO (1 atm). As soon as the dissolution of the solid was observed (aprox. 30 min) all volatiles were removed *in vacuo* and the resulting solid washed with hexane (3 x 5 mL), dried *in vacuo* and finally identified as [Ir(CO)(cod)(SiNP)]Cl ([**3**]Cl, 151 mg, 92% yield). Found: C, 59.00; H, 5.11; N, 2.68. Calcd for $C_{49}H_{52}ClIrN_2OP_2Si$ (1002.65): C, 58.70; H, 5.23; N, 2.79. ν_{CO} (CH_2Cl_2), 1994 cm^{-1}. ^1H and ^{31}P NMR spectra of a freshly prepared solution of [**3**]Cl in CD_2Cl_2 are very similar to those measured for [**3**][PF_6].

b) Formation of [IrCl(CO)(SiNP)] (**4**) and IrHCl(CO)(SiNP–H) (**5**). A suspension of IrCl(cod)(SiNP) (**2**, 220 mg, 0.226 mmol, 974.64 g/mol) in CH_2Cl_2 (5 mL) was degassed and contacted with CO (1 atm). As soon as the dissolution of the solid was observed (aprox. 30 min) CO gas was replaced by argon gas and the solution stirred for about 12 h. Finally all volatiles were removed *in vacuo* and the resulting solid washed with hexane (3 x 5 mL), dried *in vacuo* and finally identified as a mixture of [IrCl(CO)(SiNP)] (**4**, 80%) and IrHCl(CO)(SiNP–H) (**5**, 20%) (157 mg, 78% yield). Found: C, 55.15; H, 4.68; N, 3.15. Calcd for $C_{41}H_{40}ClIrN_2OP_2Si$ (894.47): C, 55.05; H, 4.51; N, 3.13.

IrCl(CO)(SiNP) (**4**): ν_{CO} (CH_2Cl_2), 2007 cm^{-1}. $^{31}P\{^1H\}$ NMR (CD_2Cl_2, 298 K): δ 63.4 (d, $^2J_{PP}$ = 30.5, P^1), 41.2 (d, $^2J_{PP}$ = 30.5, P^2). *D* (CD_2Cl_2, 298 K) = (8.58±0.03)·10^{-6} $cm^2 \cdot s^{-1}$, R_h = 5.91±0.02

Å (R_g = 5.92 Å). Selected NMR data (δ_H, bold–type, and δ_C, italics–type) are shown in the following scheme.

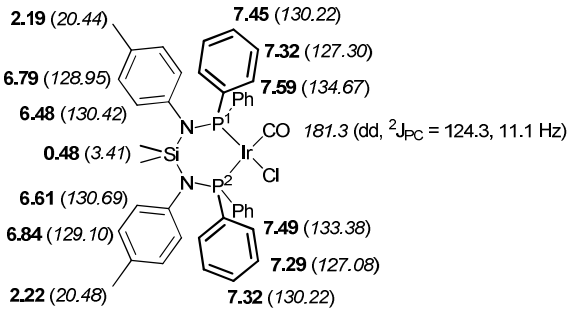

IrHCl(CO)(SiNP–H) (**5**): ν_{CO} (CH_2Cl_2), 2026 cm^{-1}. $^{31}P\{^1H\}$ NMR (CD_2Cl_2, 298 K): δ 48.1 (d, $^2J_{PP}$ = 9.0, P^1), 43.0 (d, $^2J_{PP}$ = 9.0, P^2). D (CD_2Cl_2, 298 K) = (8.45±0.11)·10^{-6} $cm^2 \cdot s^{-1}$, R_h = 6.00±0.08 Å (R_g = 6.04 Å). Selected NMR data (δ_H, bold–type, and δ_C, italics–type) are shown in the following scheme.

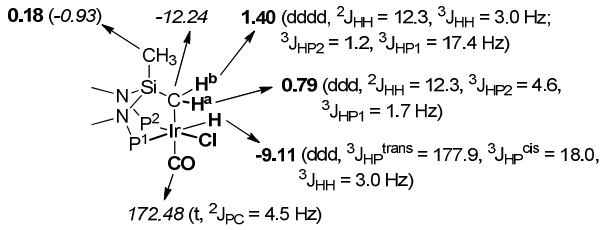

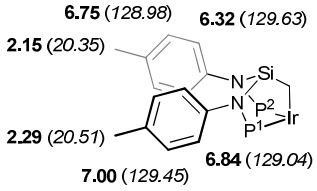

c) Synthesis of Ir(SiNP–H)$(CO)_2$ (**6**). A suspension of IrCl(cod)(SiNP) (185 mg, 0.190 mmol, 974.64 g/mol) in CH_2Cl_2 (5 mL) was degassed, contacted with CO (1 atm) and stirred at room temperature for 18 h affording a deep yellow solution. The solution was partially evaporated (aprox. 2 mL left) and layered with hexane. After 2 days, bright yellow crystals precipitated out. The supernatant solution was decanted and the crystals washed with hexane, dried *in vacuo* and identified as Ir(SiNP–H)$(CO)_2$ (**6**, 138 mg, 82% yield) Found: C, 56.02; H, 4.45; N, 3.28. Calcd for $C_{42}H_{39}IrN_2O_2P_2Si$ (886.02): C, 56.93; H, 4.44; N, 3.16. ν_{CO} (CH_2Cl_2), 2001, 1927 cm^{-1}. ^1H NMR ($CDCl_3$, 298 K): δ 7.57 (m, 4H, *o*–PPh^{endo}, δ_C = 133.87), 7.42–7.29 (10H, *o*–PPh^{exo} + *m*–

PPh^{endo} + *p*–PPh^{exo}, δ_C = 131.97, *o*–PPh, 127.56, *m*–PPh, 129.83, *p*–PPh), 7.15 (m, 4H, *m*–PPh^{exo}, δ_C = 127.41), 7.25 (m, 2H, *p*–PPh^{endo}, δ_C = 129.83), 6.84 (d, 2H, $^3J_{HH}$ = 8.1 Hz, C^3H^{tol}, δ_C = 128.86), 6.55 (d, 2H, $^3J_{HH}$ = 8.1 Hz, C^2H^{tol}, δ_C = 129.37), 2.21 (s, 6H, CH_3^{tol}, δ_C = 20.76), 0.61 (t, 2H, $^3J_{HP}$ = 10.2 Hz, $SiCH_2Ir$, δ_C = 0.14, t, $^2J_{CP}$ = 8.1 Hz), –0.36 (s, 3H, $SiCH_3$, δ_C = 26.7). $^{31}P\{^1H\}$ NMR ($CDCl_3$, 298 K): δ 49.6 (s).

X–ray measurements and structure determination of Ir(SiNP–H)$(CO)_2$ (6)

Single crystals of Ir(SiNP–H)$(CO)_2$ (**6**) were obtained by layering hexane over a CH_2Cl_2 solution of **6**. Intensities were collected at 100 K using a Bruker SMART APEX diffractometer with graphite–monochromated Mo Kα radiation (λ = 0.71073 Å) following standard procedures. Intensities were integrated and corrected for absorption effects using the SAINT+[16] and SADABS[17] programs, included in the APEX2 package. The structure was solved by standard direct methods. All non–H atoms were located in the subsequent Fourier maps. Refinement was carried out by full–matrix least–square procedure (based on F_0^2) using anisotropic temperature factors for all non–hydrogen atoms. The H atoms were placed in calculated positions with fixed isotropic thermal parameters ($1.2U_{equiv}$) of the parent carbon atom. Calculations were performed with SHELX–97[18] program implemented in the WinGX[19] package.

Crystal data for **6**: $C_{42}H_{39}IrN_2O_2P_2Si$, M = 885.98 g·mol^{-1}; pale yellow needle, 0.15 x 0.17 x 0.40 mm^3; triclinic, P–1; a = 12.007(12) Å, b = 12.770(12) Å, c = 12.878(12) Å, α = 102.208(11)º, β = 100.476(11)º, γ= 100.405(11)º; Z = 2; V = 1848(3) Å^3; D_c = 1.592 g·cm^{-3}; μ = 3.771 mm^{-1}, minimum and maximum absorption correction factors 0.416 and 0.568; $2\theta_{max}$ = 57.22º; 21576 collected reflections, 8627 unique (R_{int} = 0.0358); 8627/0/454 data/restraints/parameters; final GOF = 1.059; R1 = 0.0318 (7665 reflections, I>2σ(I)); wR2 = 0.0754 for all data. CCDC refcode 941530.

DFT geometry optimization

The molecular structures were optimized at the ONIOM(BP3LYP/GenECP:UFF) level using the Gaussian09 program.[20] The aromatic rings were included in the low level layer and the remaining atoms in the high level layer. The LanL2TZ(f) basis and pseudo potential were used for iridium and the 6–31G(d,p) basis set for the remaining atoms. Stationary points were characterized by vibrational analysis (transition states featuring one imaginary frequency, minimum energy molecular structures featuring only positive frequencies).

Associated Content

Supporting Information: Selected NMR and kinetic data, the CIF file for the structure of **6**, and the *.mol* files of the optimized structures are available free of charge via the Internet at http://pubs.acs.org.

Author Information

Corresponding author: passarel@unizar.es (V.P.), tel.: +34 976 739863.

The authors declare no competing financial interest.

Acknowledgements

Financial support from Spanish "Ministerio de Economía y Competitividad" (CTQ2010–15221) and "Diputación General de Aragón" (Group E07) is gratefully acknowledged. VP is indebted to Dr. Pablo Sanz (ISQCH, Universidad de Zaragoza) for insightful comments and useful discussions about the X–ray determination of complex **6**.

References and notes

[1] a) Carter, E; Cavell, K.; Gabrielli, W. F.; Hanton, M. J.; Hallett, A. J.; McDyre, L.; Platts, J. A.; Smith, D. M.; Murphy, D. M. *Organometallics* **2013**, *32*, 1924–1931; b) Cloete, N.; Visser, H. G.; Engelbrecht, I.; Overett, M. J.; Gabrielli, W. F.; Roodt, A. *Inorg. Chem*. **2013**, *52*, 2268–2270; c) Mayer, T.; Boettcher, H.–C. *Polyhedron* **2013**, *50*, 507–511; d) Ogawa, T.; Kajita, Y.; Wasada–Tsutsui, Y.; Wasada, H.; Masuda, H. *Inorg. Chem*. **2013**, *52*, 182–195; e) Pernik, I.; Hooper, J. F.; Chaplin, A. B.; Weller, A. S.; Willis, M. C. *ACS Catal.* **2012**, *2*, 2779–2786; f) Todisco, S.; Gallo, V.; Mastrorilli, P.; Latronico, M.; Re, N.; Creati, F.; Braunstein, P. *Inorg. Chem*. **2012**, *51*, 11549–11561; g) Do, L. H.; Labinger, J. A.; Bercaw, J. E. *Organometallics* **2012**, *31*, 5143–5149; h) Trentin, F.; Chapman, A. M.; Scarso, A.; Sgarbossa, P.; Michelin, R. A.; Strukul, G.; Wass, D. F. *Adv. Synth. Cat*. **2012**, *354*, 1095–1104; i) Bowen, L. E.; Charernsuk, M.; Hey, T. W.; McMullin, C. L.; Orpen, A. G.; Wass, D. F. *Dalton Trans*. **2012**, *39*, 560–567; j) Aluri, B.; Peulecke, N.; Muller, B. H.; Peitz, S.; Spannenberg, A.; Hapke, M.; Rosenthal, U. *Organometallics* **2012**, *29*, 226–231; k) Cheung, H. W.; So, C. M.; Pun, K. H.; Zhou, Z.; Lau, C. P. *Adv. Synth. Cat*. **2011**, *353*, 411–425; l) Gopalakrishnan, J. *Appl. Organomet. Chem.* **2009**, *23*, 291–318; m) Ozerov, O. V.; Guo, C.; Foxman, B. M. *J. Organomet. Chem*. **2006**, *691*, 4802–4806; n) Bollmann, A.; Blann, K.; Dixon, J. T.; Hess, F. M.; Killian, E.; Maumel, H.; McGuiness, D. S.; Morgan, D. H.; Neveling, A.; Otto, S.; Overett, M.; Slawin, A. M. Z.; Wasserscheid, P.; Kuhlmann, S. *J. Am. Chem. Soc*. **2004**, *126*, 14712–14713; o) Slawin, A. M. Z.; Wainwright, M.; Woolins, J. D. *J. Chem. Soc., Dalton Trans*. **2002**, 513–51.

[2] a) Aucott, S. M.; Clarke, M. L.; Slawin, A. M. Z.; Woolins, J. D. *J. Chem. Soc., Dalton Trans.* **2001**, 972–976; b) Clarke, M. L.; Slawin, A. M. Z.; Woolins, J. D. *Phosphorus Sulfur Silicon Relat. Elem.* **2001**, *168–169*, 329–332.

[3] Passarelli, V.; Benetollo, F. *Inorg. Chem*. **2011**, *50*, 9958–9967.

[4] Makino, T.; Yamamoto, Y.; Itoh, K. *Organometallics* **2004**, *23*, 1730-1737.

[5] Shibata, T.; Yamashita, K.; Ishida, H.; Takagi, K. *Org. Lett.* **2001**, *3*, 1217-1219.

[6] The calculated ν_{CO} wave number is 1998 cm^{-1} and the experimental value is 1994 cm^{-1}.

[7] Minch, M. J. *Concepts in Magn. Reson*. **1994**, *6*, 41–56.

[8] It is noteworthy that while [**3**]Cl readily react with excess of CO affording **6** after 12 h of exposure to a CO atmosphere, [**3**][PF_6] do not react with CO even after prolonged exposure to a CO atmosphere thus indicating that the presence of the chloride ion is essential in order to obtain **6**.

[9] CCDC refcode ATOQUV, in, Adams, J. J.; Arulsamy, N.; Roddick, D. M. *Organometallics* **2011**, *30*, 697–711

[10] CCDC refcode JEPTIH, in, Burrell, A. K.; Roper, W. R. *Organometallics* **1990**, 9, 1905–1910.

[11] a) Sundermann, A.; Uzan, O.; Milstein, D.; Martin, J. M. L *J. Am. Chem. Soc.* **2000**, *122*, 7095–7104; b) Rybtchinski, B.; Milstein, D.; *J. Am. Chem. Soc.* **1999**, *121*, 4528–4529; c) van

der Boom, M. E.; Liou, S.–Y.; Ben–David, Y.; Gozin, M.; Milstein, D. *J. Am. Chem. Soc.* **1998**, *120*, 13415–13421.

[12] Herde, J. L.; Lambert, J. C.; Senoff, C. V. *Inorg. Synth.* **1974**, *15*, 18–20.

[13] Day, V. W.; Klemperer, W. G.; Main, D. J. *Inorg. Chem*. **1990**, *29*, 2345–2355.

[14] a) Stilbs, P. *Prog. Nucl. Magn. Reson. Spectrosc*. 1987, 19, 1–45; b) Price, W. S. *Concepts Magn. Reson*. 1997, 9, 299–336; c) Price, W. S. *Concepts Magn. Reson*. 1998, 10, 197–237; d) Johnson, C. S. Jr., *Prog. Nucl. Magn. Reson. Spectrosc*. 1999, 34, 203–256; e) Cohen, Y.; Avram, L.; Frish, L.; *Angew. Chem*. 2005, 117, 524–560; f) Cohen, Y.; Avram, L.; Frish, L. *Angew. Chem. Int. Ed*. 2005, 44, 520–554; g) Pregosin, P. S.; Kumar, P. G. A.; Fernandez, I. *Chem. Rev*. 2005, 105, 2977–2998; h) Macchioni, A.; Ciancaleoni, G.; Zuccaccia, C.; Zuccaccia, D. *Chem. Soc. Rev*. 2008, 37, 479–489.

[15] Ortega, A.; Amoros, D.; García de la Torre, J. *Biophys. J*. **2011**, *101*, 892-898.

[16] *SAINT*+, version 6.01; Bruker AXS, Inc.; Madison, WI, 2001.

[17] Sheldrick, G. M. *SABADS*; University of Göttingen: Göttingen, Germany, 1999.

[18] a) Sheldrick, G. M. *SHELXL–97*; University of Göttingen: Göttingen, Germany, 1997; b) Sheldrick, G. M. *Acta Crystallogr.* **2008**, *A64*, 112–122.

[19] Farrugia, L. J. *J. Appl. Crystallogr*. **1999**, *32*, 837–838.

[20] Frisch, M. J. et al. Gaussian 09 (Revision A.02); Gaussian, Inc. Wallingford, CT, 2009.